

# Precise Point Positioning Using IGS Orbit and Clock Products

JAN KOUBA and PIERRE HÉROUX

*Geodetic Survey Division, Geomatics Canada, Natural Resources Canada, 615 Booth Street, Room 458A, Ottawa, Ontario K1A 0E9 Canada*

*The contribution details a post-processing approach that uses undifferenced dual-frequency pseudorange and carrier phase observations along with IGS precise orbit products, for stand-alone precise geodetic point positioning (static or kinematic) with cm precision. This is possible if one takes advantage of the satellite clock estimates available with the satellite coordinates in the IGS precise orbit products and models systematic effects that cause cm variations in the satellite to user range. This paper will describe the approach, summarize the adjustment procedure, and specify the earth- and space-based models that must be implemented to achieve cm-level positioning in static mode. Furthermore, station tropospheric zenith path delays with cm precision and GPS receiver clock estimates precise to 0.1 ns are also obtained. © 2001 John Wiley & Sons, Inc.*

## INTRODUCTION

**T**he International GPS Service (IGS) has provided GPS orbit products to the scientific community with increased precision and timeliness. Many users interested in geodetic positioning have adopted the IGS precise orbits to achieve cm-level accuracy and ensure long-term reference frame stability. Currently, a differential positioning approach that requires the combination of observations from a minimum of two GPS receivers, with at least one occupying a station with known coordinates, is commonly used. The user position can then be estimated relative to one or multiple reference stations using differenced carrier phase observations and a baseline or network estimation approach. Baseline or network processing is an effective way to cancel out common satellite/receiver

errors and to connect the user position to the coordinates of the reference stations while the precise orbit virtually eliminates the errors introduced by the GPS space segment. This mode of processing has proven to be very effective and has received widespread acceptance. One drawback is the practical constraint imposed by the requirement that simultaneous observations be made at reference stations. An attractive alternative to differential positioning is a single station positioning utilizing precise orbit/satellite solutions and undifferenced observations. Single station positioning with fixed precise orbit solutions and Doppler satellite observations was first introduced in the early 1970s by R.R. Anderle, who named the method "precise point positioning" (PPP).

The Geodetic Survey Division (GSD) of Natural Resources Canada (NRCan), formerly Energy, Mines and Resources (EMR), has been an active participant in the International GPS Service since its pilot phase in 1992. As one of seven IGS Analysis Centers known as EMR, GSD contributes daily predicted, rapid, and final GPS orbits and clocks to the IGS combinations. Recently, an ultra-rapid product to serve meteorological applications and support Low Earth Orbiter (LEO) missions has been added to the GSD's product submissions to the IGS. GSD has also played a key role in the past as the IGS Analysis Center (AC) Coordination Center and is now responsible for IGS Reference Frame Coordination, contributing together with other space techniques to the International Earth Rotation Service (IERS) realization of the International Terrestrial Reference Frame (ITRF). The daily computation of global precise GPS orbits and clocks is one way the GSD has chosen to support the Canadian Spatial Reference System (CSRS) in order to connect it into the ITRF and facilitate the integration of GPS surveys within Canada. The daily availability of data from a number of tracking stations that

are part of the Canadian Active Control System (CACS) along with precise GPS orbit products provide Canadian GPS users the opportunity to link directly into the CSRS and position themselves within a globally integrated reference frame (ITRF) with cm accuracy.

The PPP approach, with precise satellite orbit/clock solutions held fixed and undifferenced smoothed pseudoranges has been used by GSD since 1992 (Héroux, Caissy, & Gallace, 1993). For GPS users interested in meter-level positioning, a simple point positioning interface combining pseudorange data with precise orbits and clocks can be used. GSD uses 30-s tracking data from selected IGS stations with stable atomic clocks (Héroux & Kouba, 1995) and precise IGS satellite clocks at 15-min intervals to produce 30-s precise satellite clocks. These products satisfy GPS users observing at high data rates in either static or kinematic modes for applications requiring meter precision. For GPS users seeking to achieve geodetic precision, sophisticated processing software such as GIPSY (Lichten et al., 1995), BERNESE (Rothacher & Mervart, 1996), and GAMIT (King & Bock, 1999) are required. By using the IGS precise orbit products and combining the GPS carrier phase data with CACS observations, geodetic users achieve precise positioning while integrating into the CSRS. Software provided by receiver manufacturers may also be used as long as it allows for the input of station and orbit data in standard format.

For a number of years, PPP (Zumberge et al., 1997) algorithms using undifferenced carrier phase observations have also been available in the GIPSY (Lichten et al., 1995) GPS analysis software. More recently, they have been added to the traditional double-differencing BERNESE software (Rothacher & Mervart, 1996). Users now have the option of processing data from a single station to obtain positions with cm precision within the reference frame provided by the IGS orbit products. NRCan PPP software also evolved from its original version (Héroux et al., 1993) to provide increasing precision. Point positioning eliminates the need to acquire simultaneous tracking data from a reference (base) station or a network of stations. It has given rise to centralized geodetic positioning services that require from the user the simple submission of a request and a valid GPS observation file (see, e.g., Zumberge, 1999). The approach presented here is an implementation of precise point positioning that effectively distributes processing by providing portable software that can be used on a personal computer and takes advantage of the highly accurate global reference frame made available through the IGS orbit products.

## THE IGS GPS ORBIT PRODUCTS

The IGS Precise Orbit products come in various flavors, from the Final, Rapid, and Predicted to the unofficial Ultra-Rapid. They differ mainly by their varying latency and the extent of the tracking network used for their computation. The IGS Final orbits are combined from up to seven contributing IGS Analysis Centers (ACs) and are usually available on the 11th day after the last observation. The Rapid orbit product is combined 17 hours after the end of the day of interest. The latency is mainly due to the varying availability of tracking data from stations of the global IGS tracking network, which use a variety of data acquisition and communication schemes. In the past, the IGS products have been based on a daily model that required submissions of files containing tracking data for 24-h periods. Recently, Data Centers have been asked to forward hourly tracking data to accelerate product delivery. This new submission scheme was required for the creation of an Ultra-Rapid product, with a latency of only a few hours, that should satisfy the more demanding needs of the meteorological community and future LEO (Low Earth Orbiter) missions. It is expected that IGS products will continue to be delivered with increased timeliness in the future (Kouba, Mireault, Beutler, & Springer, 1998; Neilan, Zumberge, Beutler, & Kouba, 1997).

Regarding the IGS orbit precision, one can see that over the past eight years (Figure 1) the quality of the IGS Final orbits has improved from about 30 cm to the 3–5-cm precision level currently realized by some of the ACs (Kouba, 1998). It is also interesting to note that the Rapid orbit combined product is as precise as the best AC Final solution with less tracking stations and faster delivery time. This fact confirms the belief that increasing the number of global GPS tracking stations does not necessarily translate into higher orbit precision. One element that has not yet received much attention is the quality of the GPS satellite clock estimates included in the IGS orbit products. Examining the IGS Final summary reports (<http://igs.cb.jpl.nasa.gov/mail/igsreports/>) produced weekly by the IGS AC coordinator (Dr. R. Weber, Astronomical Institute, University of Berne), we notice that satellite clock estimates produced by different ACs agree within 0.1–0.2-ns RMS, or 3–6 cm, a level compatible with the orbit precision. The combination of precise GPS orbits and clocks, weighted according to their corresponding sigmas, is essential for PPP, given that the proper measurements are made at the user set and the observation models are correctly implemented.

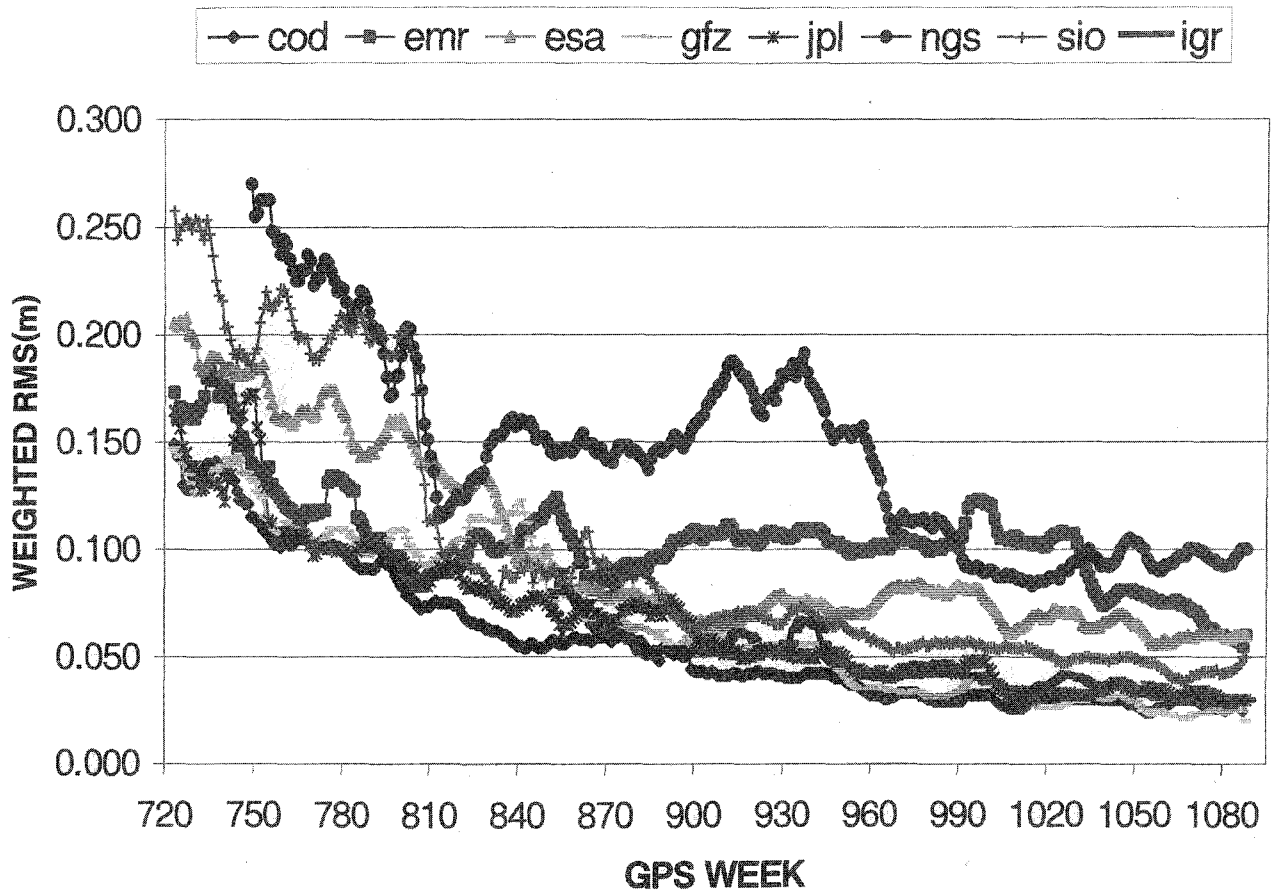


**FIGURE 1. Weighted orbit RMS of the IGS rapid and AC final orbit solutions with respect to the IGS final orbit products. COD: Center for Orbit Determination in Europe, AIUB, Switzerland; EMR: Natural Resources Canada, Canada; ESA: European Space Operations Center, ESOC, Germany; GFZ: GeoForschungsZentrum, Germany; JPL: Jet Propulsion Laboratory, USA; NGS: National Oceanic and Atmospheric Administration/NOAA, USA; SIO: Scripps Institution of Oceanography, USA; IGR: IGS Rapid Orbit Combinations.**

## PRECISE POINT POSITIONING

### Observation Equations

The ionosphere-free combinations of dual-frequency GPS pseudorange (P) and carrier phase observations ( $\Phi$ ) are related to user position, clock, troposphere, and ambiguity parameters according to the following simplified observation equations:

$$\ell_P = \rho + c(dt - dT) + T_r + \varepsilon_P \quad (1)$$

$$\ell_\Phi = \rho + c(dt - dT) + N\lambda + \varepsilon_\Phi \quad (2)$$

where:

$\ell_P$  is the ionosphere-free combination of L1 and L2 pseudoranges ( $2.54P_1 - 1.54P_2$ ),

$\ell_\Phi$  is the ionosphere-free combination of L1 and L2 carrier phases ( $2.54\phi_1 - 1.54\phi_2$ ),

$dt$  is the station receiver clock offset from GPS time,

$dT$  is the satellite clock offset from GPS time,

$c$  is the vacuum speed of light,

$T_r$  is the signal path delay due to the neutral-atmosphere (primarily the troposphere),

$\lambda$  is the carrier, or carrier combination, wavelength,

$N$  is the non-integer ambiguity of the carrier phase ionosphere-free combination, and

$\varepsilon_P, \varepsilon_\Phi$  are the relevant measurement noise components, including multipath.

Symbol  $\rho$  is the geometrical range computed as a function of satellite ( $X_s, Y_s, Z_s$ ) and station ( $x, y, z$ ) coordinates according to:

$$\rho = \sqrt{(X_s - x)^2 + (Y_s - y)^2 + (Z_s - z)^2}$$

Expressing the tropospheric path delay ( $T_r$ ) as a function of the zenith path delay ( $zpd$ ) with mapping function ( $M$ ), relating the tropospheric delay to the elevation angle of the satellite, while removing the known satellite clocks ( $dt$ ) gives the following mathematical model in the simplest form:

$$f_p = \rho + c dt + M zpd + \varepsilon_p - \ell_p = 0 \quad (3)$$

$$f_\phi = \rho + c dt + M zpd + N\lambda + \varepsilon_\phi - \ell_\phi = 0 \quad (4)$$

$$A = \begin{bmatrix} \frac{\partial f(X, \ell_p)}{\partial x} & \frac{\partial f(X, \ell_p)}{\partial y} & \frac{\partial f(X, \ell_p)}{\partial z} & \frac{\partial f(X, \ell_p)}{\partial dt} & \frac{\partial f(X, \ell_p)}{\partial zpd} & \frac{\partial f(X, \ell_p)}{\partial N_{(j=1, nsat)}} \\ \frac{\partial f(X, \ell_\phi)}{\partial x} & \frac{\partial f(X, \ell_\phi)}{\partial y} & \frac{\partial f(X, \ell_\phi)}{\partial z} & \frac{\partial f(X, \ell_\phi)}{\partial dt} & \frac{\partial f(X, \ell_\phi)}{\partial zpd} & \frac{\partial f(X, \ell_\phi)}{\partial N_{(j=1, nsat)}} \end{bmatrix}$$

with

$$X^T = [x \ y \ z \ dt \ zpd \ N_{(j=1, nsat)}^j].$$

The least squares solution with a priori weighted constraints ( $P_X$ ) to the parameters is given by:

$$\delta = -(P_X^0 + A^T P_\ell A)^{-1} A^T P_\ell W, \quad (5)$$

so that the estimated parameters are

$$\bar{X} = X^0 + \delta,$$

with covariance matrix

$$C_{\bar{X}} = P_{\bar{X}}^{-1} = (P_X^0 + A^T P_\ell A)^{-1}. \quad (6)$$

## Adjustment Procedure

The adjustment procedure developed is effectively a sequential filter that adapts to varying user dynamics. The implementation considers the variations in the states of the parameters between observation epochs and uses appropriate stochastic processes to update their variances. The current model involves four types of parameters: station position ( $x, y, z$ ), receiver clock ( $dt$ ), troposphere zenith path delay ( $zpd$ ), and carrier phase ambiguities ( $N$ ). The station position may be constant or change over time depending

## Adjustment Model

Linearization of observation equations (3) and (4) around the a priori parameters and observations ( $X^0, \ell$ ) becomes, in matrix form:

$$A\delta + W - V = 0,$$

where  $A$  is the design matrix,  $\delta$  is the vector of corrections to the unknown parameters  $X$ ,  $W = f(X^0, \ell)$  is the misclosure vector, and  $V$  is the vector of residuals.

The partial derivatives of the observation equations with respect to  $X$ , consisting of four types of parameters: station position ( $x, y, z$ ), clock ( $dt$ ), troposphere zenith path delay ( $zpd$ ), and (non-integer) carrier phase ambiguities ( $N$ ), form the design matrix  $A$ :

on the user dynamics. These dynamics could vary from tens of meters per second in the case of a land vehicle to a few kilometers per second for a low earth orbiter (LEO). The receiver clock will drift according to the quality of its oscillator, e.g., several cm/s in the case of an internal quartz clock with frequency stability of about  $10^{-10}$ . Comparatively, the zenith path delay will vary in time by a relatively small amount, in the order of a few cm/h. Finally, the non-integer carrier phase ambiguities ( $N$ ) will remain constant as long as the carrier phases are free of cycle slips, a condition that requires close monitoring. [Note that only for double differenced data is  $dt$  practically eliminated and the carrier phase ambiguities ( $N$ ) become integers.]

Using subscript  $i$  to denote a specific time epoch, we see that without observations between epochs, initial parameter estimates at epoch  $i$  are equal to the ones obtained at epoch  $i-1$ :

$$X_i^0 = \bar{X}_{i-1}. \quad (7)$$

To propagate the covariance information from epoch  $i-1$  to  $i$ , during an interval  $\Delta t$ ,  $C_{\bar{X}_{i-1}}$  has to be updated to include process noise represented by the covariance matrix  $C_{E_{\Delta t}}$ :

$$P_{X_i^0} = [C_{\bar{X}_{i-1}} + C_{E_{\Delta t}}]^{-1} \quad (8)$$

where

$$C\mathcal{E}_{\Delta t} = \begin{bmatrix} C\mathcal{E}(x)_{\Delta t} & 0 & 0 & 0 & 0 & 0 \\ 0 & C\mathcal{E}(y)_{\Delta t} & 0 & 0 & 0 & 0 \\ 0 & 0 & C\mathcal{E}(z)_{\Delta t} & 0 & 0 & 0 \\ 0 & 0 & 0 & C\mathcal{E}(dt)_{\Delta t} & 0 & 0 \\ 0 & 0 & 0 & 0 & C\mathcal{E}(zpd)_{\Delta t} & 0 \\ 0 & 0 & 0 & 0 & 0 & C\mathcal{E}(N_{(j=1, nsat)}^j)_{\Delta t} \end{bmatrix}$$

Process noise can be adjusted according to user dynamics, receiver clock behavior, and atmospheric activity. In all instances  $C\mathcal{E}(N_{(j=1, nsat)}^j)_{\Delta t} = 0$  since the carrier phase ambiguities remain constant over time. In static mode, the user position is also constant and consequently  $C\mathcal{E}(x)_{\Delta t} = C\mathcal{E}(y)_{\Delta t} = C\mathcal{E}(z)_{\Delta t} = 0$ . In kinematic mode, it is increased as a function of user dynamics. The receiver clock process noise can vary as a function of frequency stability but is usually set to white noise with a large  $C\mathcal{E}(dt)_{\Delta t}$  value to accommodate the unpredictable occurrence of clock resets. A random walk process noise of  $5 \text{ mm}/\sqrt{\text{h}}$  is assigned to the zenith path delay  $C\mathcal{E}(zpd)_{\Delta t}$ .

## PRECISE POINT POSITIONING CORRECTION MODELS

Developers of GPS software are generally well aware of corrections they must apply to pseudorange or carrier phase observations to eliminate effects such as special and general relativity, Sagnac delay, satellite clock offsets, atmospheric delays, etc. (e.g., ION, 1980). All these effects are quite large, exceeding several meters, and must be considered even for pseudorange positioning at the meter precision level. When attempting to combine satellite positions and clocks precise to a few centimeters with ionospheric-free carrier phase observations (with millimeter resolution), it is important to account for some effects that may not have been considered in pseudorange or precise differential phase processing modes.

The following sections look at additional correction terms that are significant for carrier phase point positioning. They have been grouped under “Satellite Attitude Effects,” “Site Displacements Effects,” and “Compatibility Considerations.” A number of the corrections listed below require the Moon or the Sun positions, which can be obtained from readily available planetary ephemerides files, or more conveniently from simple formulas (as implemented here) since a relative precision of about  $1/1000$  is sufficient for corrections at the millimeter precision level. Note that for centimeter-level differential positioning and baselines of less than 100 km, the correction terms discussed below can be safely neglected.

## Satellite Attitude Effects

### Satellite antenna offsets

The requirement for satellite-based corrections originates from the separation between the GPS satellite center of mass and the phase center of its antenna. Because the force models used for satellite orbit modeling refer to its center of mass, the IGS GPS precise satellite coordinates and clock products also refer to the satellite center of mass, unlike the orbits broadcast in the GPS navigation message that refer to satellite antenna phase center. However, the measurements are made to the antenna phase center; thus one must know satellite phase center offsets and monitor the orientation of the offset vector in space as the satellite orbits the Earth. The phase centers for most satellites are offset both in the body z-coordinate direction (toward the Earth) and in the body x-coordinate direction, which is on the plane containing the Sun (see Figure 2).

### Phase wind-up correction

GPS satellites transmit right circularly polarized (RCP) radio waves, and therefore the observed carrier phase depends on the mutual orientation of the satellite and receiver antennas. A rotation of either receiver or satellite antenna around its bore (vertical) axis will change the carrier phase up to one cycle (one wavelength), which corresponds to one complete revolution of the antenna. This effect is called “phase wind-up” (Wu et al., 1993). A receiver antenna, unless mobile, does not rotate around its vertical axis and it is oriented toward a reference azimuth direction (usually north). However, satellite antennas undergo slow rotations (around vertical axes) as their solar panels are being oriented toward the Sun and the station-satellite geometry changes. Besides, during eclipsing seasons, satellites are also subjected to rapid rotations, so-called “noon” (when a straight line, starting from the Sun, intersects the satellite and then the center of the Earth) and “midnight turns” (when the line from the Sun intersects the center of the Earth, then the

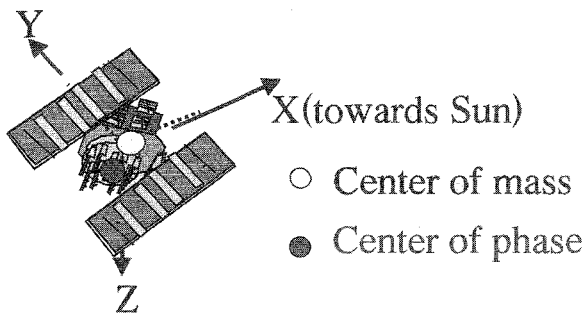


**FIGURE 2. IGS conventional antenna phase center in satellite fixed reference frame (m). Block II/IIA  $X = 0.279$ ,  $Y = 0.000$ ,  $Z = 1.023$ ; Block IIR  $X = 0.000$ ,  $Y = 0.000$ ,  $Z = 0.000$ .**

satellite), to reorient their solar panels toward the Sun. This can represent antenna rotations of up to one revolution within less than 30 min. During such noon or midnight turns, phase data needs to be corrected for this effect (Bar-Sever, 1996), or simply edited out.

The phase wind-up correction has been generally neglected even in the most precise differential positioning software, as it is quite negligible for double-difference positioning on baselines/networks spanning up to a few hundred kilometers—although it has been shown that it can reach up to 4 cm for a baseline of 4000 km (Wu et al., 1993). However, this effect is quite significant for undifferenced point positioning when fixing IGS satellite clocks because it can reach up to one half of the wavelength. Since about 1994, most of the IGS Analysis Centers (and therefore the combined IGS orbit/clock products) apply this phase wind-up correction. Neglecting it and fixing IGS orbits/clocks will result in position and clock errors at the dm level. For receiver antenna rotations (e.g., during kinematic positioning/navigation) phase wind-up is fully absorbed into station clock solutions (or eliminated by double differencing).

The phase wind-up correction can be evaluated from dot ( $\cdot$ ) and vector ( $\times$ ) products according to Wu et al. (1993) as follows:

$$\delta\phi = \text{sign}(\zeta) \cos^{-1}(\bar{D}' \cdot \bar{D} / |\bar{D}'| |\bar{D}|), \quad (9)$$

where  $\zeta = \bar{k} \cdot (\bar{D}' \times \bar{D})$ ,  $\bar{k}$  is the satellite-to-receiver unit vector and  $\bar{D}'$ ,  $\bar{D}$  are the effective dipole vectors of the satellite and receiver computed from the current satellite

body coordinate unit vectors ( $\bar{x}'$ ,  $\bar{y}'$ ,  $\bar{z}'$ ) and the local receiver unit vectors north, east, and up ( $\bar{x}$ ,  $\bar{y}$ ,  $\bar{z}$ ).

$$\bar{D}' = \bar{x}' - \bar{k}(\bar{k} \cdot \bar{x}') - \bar{k} \times \bar{y}',$$

$$\bar{D} = \bar{x} - \bar{k}(\bar{k} \cdot \bar{x}) + \bar{k} \times \bar{y}.$$

Continuity between consecutive phase observation segments must be ensured by adding full cycle terms of  $\pm 2\pi$  to the correction (9).

### Site Displacements Effects

In a global sense, a station undergoes real or apparent periodic movements reaching a few dm that are not included in the corresponding ITRF position. Consequently, if one is to obtain a precise station coordinate solution consistent with the current ITRF conventions, the above station movements must be modeled by adding the site displacement correction terms listed below to the conventional ITRF coordinates. Effects with magnitude of less than 1 cm such as atmospheric and snow build-up loading have not been considered in the following.

### Solid Earth tides

The “solid” Earth is in fact pliable enough to respond to the same gravitational forces that generate the ocean tides. The periodic vertical and horizontal site displacements caused by tides are represented by spherical harmonics of degree and order ( $n m$ ) characterized by the Love number  $h_{nm}$  and the Shida number  $l_{nm}$ . The effective values of these numbers weakly depend on station latitude and tidal frequency (Wahr, 1981) and need to be taken into account when an accuracy of 1 mm is desired in determining station positions (see, e.g., IERS, 1996). However, for 5-mm precision, only the second-degree tides and a height correction term are necessary.

For the site displacement vector in Cartesian coordinates  $\Delta \vec{r}^T = [\Delta x \ \Delta y \ \Delta z]$  (IERS, 1989):

$$\Delta \vec{r} = \sum_{j=2}^3 \frac{GM_j}{r_j^2} \frac{r^4}{R_j^3} \left[ \left[ 3l_2(\bar{R}_j \cdot \bar{r}) \right] \bar{R}_j + 3 \left( \frac{h_2}{2} - l_2 \right) (\bar{R}_j \cdot \bar{r})^2 - \frac{h_2}{2} \right] \bar{r} + [-0.025 \sin\phi \cos\phi \sin(\theta_g + \lambda)] \bar{r} \quad (10)$$

where  $GM$ ,  $GM_j$  are the gravitational parameters of the Earth, the Moon ( $j = 2$ ), and the Sun ( $j = 3$ );  $r$ ,  $R_j$  are geocentric distances of the station, the Moon, and the Sun with the corresponding unit vectors  $\bar{r}$  and  $\bar{R}_j$ , respectively;  $l_2$  and  $h_2$  are the nominal second-degree Love and

Shida dimensionless numbers (0.609, 0.085);  $\phi$ ,  $\lambda$  are the site latitude and longitude (positive east) and  $\theta_g$  is Greenwich Mean Sidereal Time. The tidal correction (10) can reach about 30 cm in the radial and 5 cm in the horizontal direction. It consists of a latitude-dependent permanent displacement and a periodic part with predominantly semidiurnal and diurnal periods of changing amplitudes. The periodic part is largely averaged out for static positioning over a 24-h period. However, the permanent part, which can reach up to 12 cm in mid-latitudes (along the radial direction) remains in such a 24-h average position. The permanent tidal distortion, according to the ITRF convention (IERS, 1996), has to be used as well. In other words, the complete correction (10), which includes both the permanent and periodical tidal displacements, must be applied to be consistent with the ITRF convention. Even when averaging over long periods, neglecting the correction (10) in point positioning would result in systematic position errors of up to 12.5 and 5 cm in the radial and north directions, respectively. Note that for differential positioning over short baseline (<100 km), both stations have almost identical tidal displacements so that the relative positions over short baselines will be largely unaffected by the solid Earth tides. If the tidal displacements in the north, east, and vertical directions are required, they can be readily obtained by multiplying (10) by the respective unit vectors.

### ***Ocean loading***

Ocean loading is similar to solid Earth tides as it is dominated by diurnal and semidiurnal periods, but it results from the load of the ocean tides. While ocean loading is almost an order of magnitude smaller than solid Earth tides, it is more localized, and, by convention, it does not have a permanent part. For single epoch positioning at the 5-cm precision level, or mm static positioning over a 24-h period and/or for stations that are far from the oceans, ocean loading can be safely neglected. On the other hand, for cm-precise kinematic point positioning or precise static positioning along coastal regions over intervals significantly shorter than 24 h, this effect has to be taken into account. Note that when the tropospheric zpd or clock solutions are required, the ocean load effects also have to be taken into account even for a 24-h static point positioning processing, unless the station is far (>1000 km) from the nearest coast line. Otherwise, the ocean load effects will map into the tropospheric zpd/clock solutions (Dragert, James, & Lambert, 2000), which may be significant particularly for the coastal stations.

The ocean load effects can be modeled in each principal direction by the following correction term (IERS, 1996):

$$\Delta c = \sum_j f_j A_{cj} \cos(\omega_j t + \chi_j + u_j - \Phi_{cj}), \quad (11)$$

where  $f_j$  and  $u_j$  depend on the longitude of lunar node (at 1–3-mm precision  $f_j = 1$  and  $u_j = 0$ ); the summation of  $j$  represents the 11 tidal waves designated as  $M_2$ ,  $S_2$ ,  $N_2$ ,  $K_2$ ,  $K_1$ ,  $O_1$ ,  $P_1$ ,  $Q_1$ ,  $M_f$ ,  $M_m$ , and  $S_{sa}$ ;  $\omega_j$  and  $\chi_j$  are the angular velocity and the astronomical arguments at time  $t = 0$  h, corresponding to the tidal wave component  $j$ . The arguments  $\chi_j$  can be readily evaluated by a FORTRAN routine *ARG* available from the IERS Convention ftp site: <ftp://maia.usno.navy.mil/conventions/chapter7/arg.f>.

The station specific amplitudes  $A_{cj}$  and phases  $\Phi_{cj}$  for the radial, south (positive), and west (positive) directions are computed by convolution of Green functions utilizing the latest global ocean tide models as well as refined coastline database (e.g., Scherneck, 1991; Pagiatakis, 1992; Agnew, 1996). A table of the amplitudes  $A_{cj}$  and phases  $\Phi_{cj}$  for most ITRF stations, computed by Scherneck (1993), is also at <ftp://maia.usno.navy.mil/conventions/chapter7/olls25.bld>. Alternatively, software for evaluation of  $A_{cj}$  and  $\Phi_{cj}$  at any site is available from Pagiatakis (1992). Typically, the  $M_2$  amplitudes are the largest and do not exceed 5 cm in the radial and 2 cm in the horizontal directions for coastal stations. For cm accuracy it is also necessary to augment the global tidal model with local ocean tides digitized, for example, from the local tidal charts. Future ITRF convention will likely also require a model for the geocenter variation (at the cm level), which is also of tidal origin. Consequently the station specific amplitude  $A_{cj}$  and phases  $\Phi_{cj}$  would then include the geocenter (tidal) variation. In fact, the IERS tabulation at the above ftp site already includes the tidal geocenter variation. One consequence of this new convention/approach is that for cm station position precision, the ocean load effect corrections must be included at all stations, even for those far from the ocean.

### ***Earth rotation parameters (ERP)***

The Earth rotation parameters (i.e., Pole position  $X_p$ ,  $Y_p$ , and *UT1-UTC*), along with the conventions for sidereal time, precession, and nutation facilitate accurate transformations between terrestrial and inertial reference frames that are required in global GPS analysis (see, e.g., IERS, 1996). Then, the resulting orbits in the terrestrial conventional reference frame (ITRF), like the IGS orbit products,

imply, quite precisely, the underlying ERP. Consequently, IGS users who fix or heavily constrain the IGS orbits and work directly in ITRF need not worry about ERP. However, when using software formulated in an inertial frame, the ERP corresponding to the fixed orbits are required.

For point positioning processing formulated within the terrestrial frame, with the AC orbits held fixed, the so called sub-daily ERP model, which is also dominated by diurnal and sub-diurnal periods of ocean tide origin, may still be required to attain sub-cm positioning precision. This results from the IERS convention for ERP, i.e., the IERS/IGS ERP series as well as ITRF positions do not include the sub-daily ERP variations, which can reach up to 3 cm at the surface of the Earth. However, the IGS orbits imply the complete ERP removed, i.e., the conventional ERP plus the sub-daily ERP model. In order to be consistent, in particular for precise static positioning over intervals much shorter than 24 h, this sub-daily effect may have to be taken into account. Note that, much like the ocean tide loading, the sub-daily ERP are averaged out to nearly zero over a 24-h period.

This effect can be modeled, like all the tidal displacements, as apparent corrections ( $\Delta x$ ,  $\Delta y$ ,  $\Delta z$ ) to the conventional (ITRF) station coordinates ( $x$ ,  $y$ ,  $z$ ). It can be evaluated from the instantaneous sub-daily ERP corrections ( $\delta X_p$ ,  $\delta Y_p$ ,  $\delta UT1$ ) and the standard coordinate transformation (using the IERS convention and the rotation parameters  $R_x = \delta Y_p$ ,  $R_y = \delta X_p$ ,  $R_z = -\delta UT1$ ), i.e.,

$$\Delta x = +y \cdot \delta UT1 + z \cdot \delta X_p, \quad (12)$$

$$\Delta y = -x \cdot \delta UT1 - z \cdot \delta Y_p, \quad (13)$$

$$\Delta z = -x \cdot \delta X_p + y \cdot \delta Y_p, \quad (14)$$

where each of the sub-daily ERP component corrections ( $\delta X_p$ ,  $\delta Y_p$ ,  $\delta UT1$ ) is obtained from the following approximation form, e.g., for the  $X_p$  pole component:

$$\delta X_p = \sum_{j=1}^8 F_j \sin \xi_j + G_j \cos \xi_j. \quad (15)$$

where  $\xi_j$  is the astronomical argument at the current epoch for the tidal wave component  $j$  of the eight diurnal tidal waves considered ( $M_2$ ,  $S_2$ ,  $N_2$ ,  $K_2$ ,  $K_1$ ,  $O_1$ ,  $P_1$ ,  $Q_1$ ), augmented with  $n \cdot \pi/2$  ( $n = 0, 1, \text{ or } -1$ ) and  $F_j$  and  $G_j$  are the tidal wave coefficients derived from the latest global ocean tide models for each of the three ERP components. The above (conventional) FORTRAN routine, evaluating the sub-daily ERP corrections can also be obtained at the

(IERS, 1996) ftp site: <ftp://maia.usno.navy.mil/conventions/chapter8/ray.f>.

## Compatibility Considerations

Positioning and GPS analyses that constrain or fix any external solutions/products need to apply consistent orbit/clock weighting, models, and conventions. This is in particular true for precise point positioning and clock solutions/products. However, even for cm differential positioning, consistency with the IGS global solutions needs to be considered. This includes issues such as the respective version of ITRF, the IGS ERP, the IGS orbit, and station solutions used, the station logs (antenna offsets) and the adopted antenna calibration table (IGS\_01.pcv) available at the IGS Central Bureau (<http://igs.cb.jpl.nasa.gov>).

The GPS system already has some well developed conventions, e.g., that only the periodic relativity correction

$$\Delta T_{rel} = -2\vec{X}_s \cdot \vec{V}_s/c^2 \quad (16)$$

is to be applied by all GPS users (ION, 1980). Here  $\vec{X}_s$  and  $\vec{V}_s$  are the satellite position and velocity vectors and  $c$  is the speed of light. The same convention has also been adopted by IGS, i.e., all the IGS satellite clock solutions are consistent with this convention.

By an agreed convention, there are no group delay calibration corrections applied for the station and satellite (L2-L1) biases in all the IGS AC analyses, thus no such calibrations are to be applied when the IGS clock products are held fixed or constrained in dual-frequency point positioning. Furthermore, a specific set of pseudorange observations consistent with the IGS clock products needs to be used even for point positioning utilizing phase observations; otherwise the clock solutions are significantly affected. This is a result of significant satellite-dependent differences between L1 C/A ( $P_{C/A}$ ) and P ( $P_1$ ) code pseudoranges, which can reach up to 2 ns (60 cm). IGS has been using the following conventional pseudorange observation set, which needs to be enforced when using the IGS orbit/clock products (*IGS Mail #2744*):

Up to 02 April 2000 (GPS Week 1056):  $P_{C/A}$  and  $P'_2 = P_{C/A} + (P_2 - P_1)$

After 02 April 2000 (GPS Week 1056):  $P_1$  and  $P_2$

Note that, in the case of C/A and P-code carrier phase observations, there is no such problem, and no need for any such convention. The GPS system specifications state



that the difference between the two types of phase observation on L1 is the same for all satellites and is equal to a constant fraction of the L1 wavelength. Unlike pseudoranges, the C/A and P-code carrier phase offset is the same for all satellites and fully absorbed by the initial non-integer phase ambiguities, or completely eliminated by double differencing. For more information on this convention and how to form the above pseudorange observation set for receivers, which do not give all the necessary observation types, see *IGS Mail #2744* available from the IGS CB Archives: <http://igs.cb.jpl.nasa.gov/mail/igsmail/2000/>.

### PRECISE POINT POSITIONING (PPP) EVALUATION

All the above correction models except for ocean and atmospheric loading and sub-daily ERP effects were implemented, including satellite/clock weighting, in a program that runs on a personal computer. To evaluate our PPP implementation, daily sessions of dual-frequency code and carrier observations from globally distributed IGS stations were processed for GPS week 1039 (5–11 December 1999). Observations every 30 s were used to facilitate cycle slip detection. Station positions, clock off-

sets, and troposphere zenith path delays as well as phase ambiguity parameters were estimated at 15-min intervals (corresponding to the epochs of available precise orbits and clocks in the IGS and AC orbit/clock products).

This section shows the parameter convergence of the PPP solution and evaluates the quality of the positions, tropospheric zpds, and station clocks obtained.

### PPP Solution Convergence

PPP convergence as a function of time depends on initial parameter variances and the synergy of GPS pseudorange and carrier phase observations. At the initial epoch, because of unknown carrier phase ambiguities, the solution relies entirely on the pseudorange observations and the quality of the position reflects GPS receiver pseudorange data noise and the multipath environment at the tracking station. As time passes and phase observations are added to the solution, the ionospheric free ambiguities and station position components (in static mode) converge to constant values while the tropospheric zpd and receiver clock parameters vary as a function of their assigned process noise. Figure 3 shows a daily plot of posi-

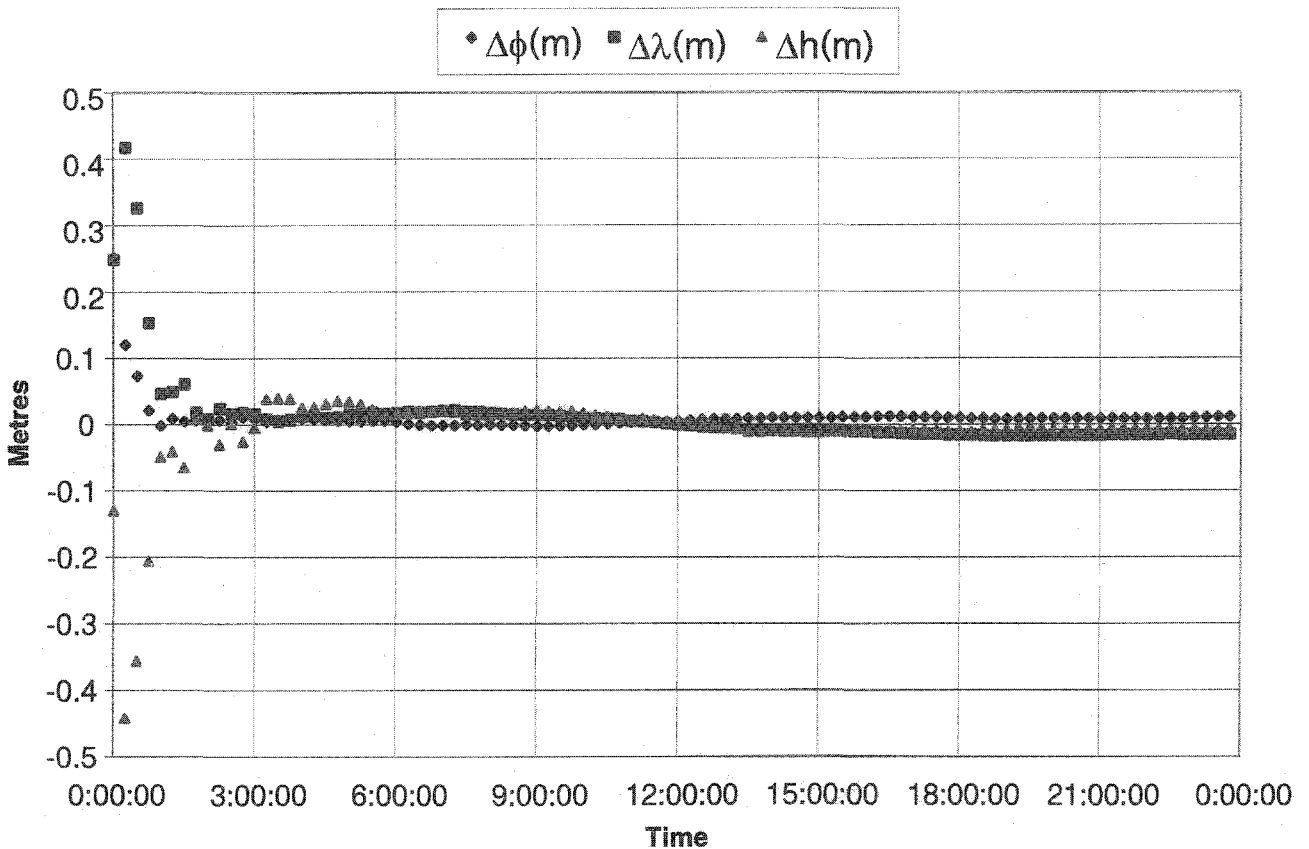


**FIGURE 3. Precise point positioning solution convergence, ALGO, 10 December 1999.**

tion parameter updates at 15-min intervals. For this particular site, initial station coordinates differ from the known values by as much as 50 cm. Considering the latitude, longitude and height differences ( $\Delta\phi$ ,  $\Delta\lambda$ ,  $\Delta h$ ) as a function of time, we notice that cm convergence is reached after processing 8–12 epochs or 2–3 h of observations. With high-rate satellite clocks every 30 s, this convergence time can be further reduced to less than 30 min.

### PPP Station Coordinates Precision Evaluation

Data for each day of GPS week 1039 (5–11 December 1999) was processed using up to 40 globally distributed GPS stations with tracking data of acceptable quality and continuity. The subset was selected from the 51 stations used by IGS for ITRF97 realization (Ferland, 2000). ITRF97 position estimates were used for comparison because they are very precise (sub-cm). Daily differences in  $x$ ,  $y$ , and  $z$  were computed using Final orbit/clock files from 3 IGS Analysis Centers (EMR, GFZ and JPL) and the IGS Rapid and Final combined orbit/clock products (IGR, IGS). Figure 4 shows differences between the posi-

tion estimates and the ITRF97 values for the 40 stations processed on 11 December 1999. Results obtained using EMR [Figure 4(a)] and IGS Final orbits [Figure 4(b)] were selected to illustrate that differences of several cm are still present in positions estimated using the orbits from certain ACs. It is also apparent that these coordinate differences are globally consistent for a specific day, that they correspond to “apparent geocenter offsets,” and that they are greatly reduced through the IGS combination process. Real geocenter motions are expected to be less than 1 cm (Dong et al., 1997). This reduction is thus evidence that there is some independence in the mismodeling by different ACs.

Table 1 gives average Cartesian coordinate differences and standard deviations for all stations and days of GPS week 1039. For all seven days, average differences are consistent at the cm-level for all analysis centers except EMR, for which  $\Delta z$  daily bias varies by as much as 20 cm during this particular week. Nevertheless, in terms of precision, we see fairly stable daily standard deviations about the mean for all ACs over the entire week. It is

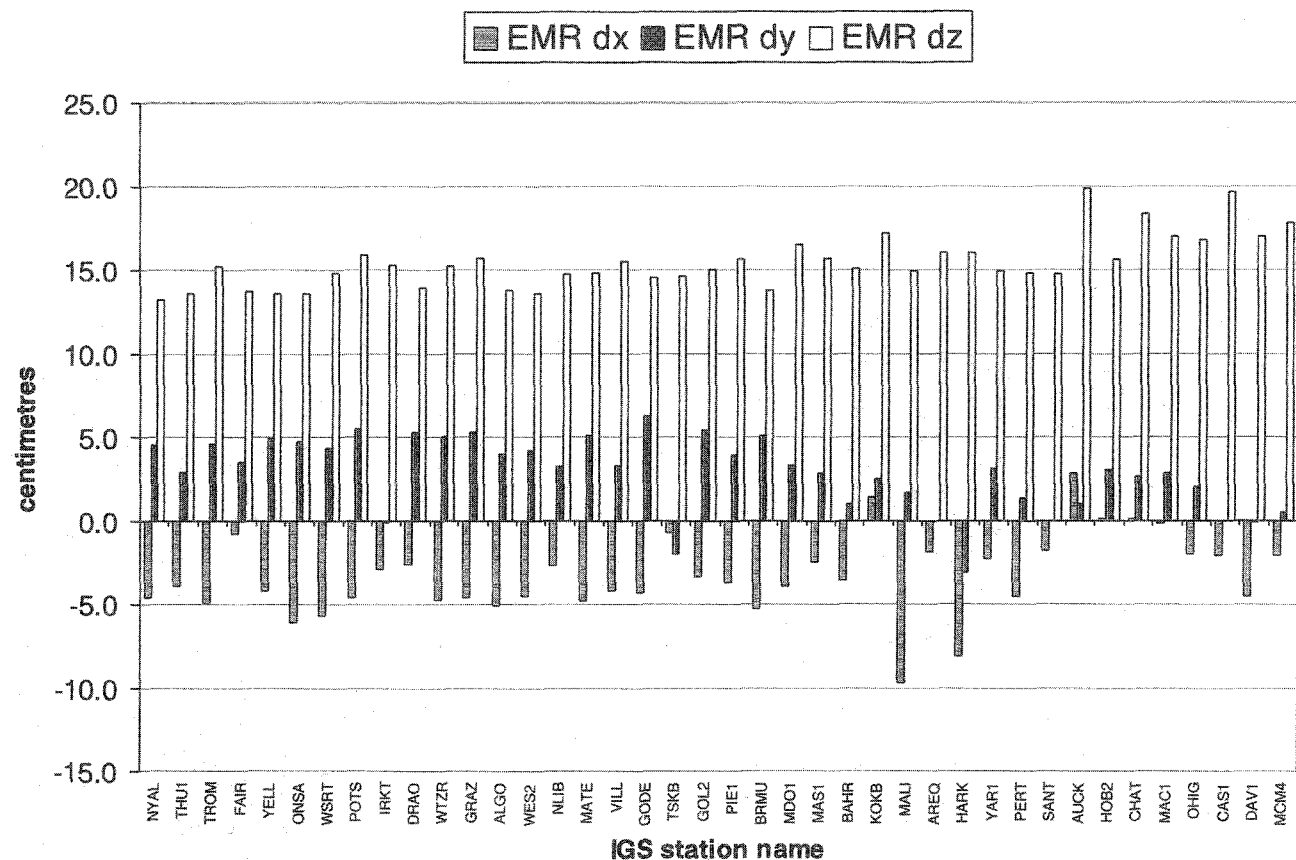
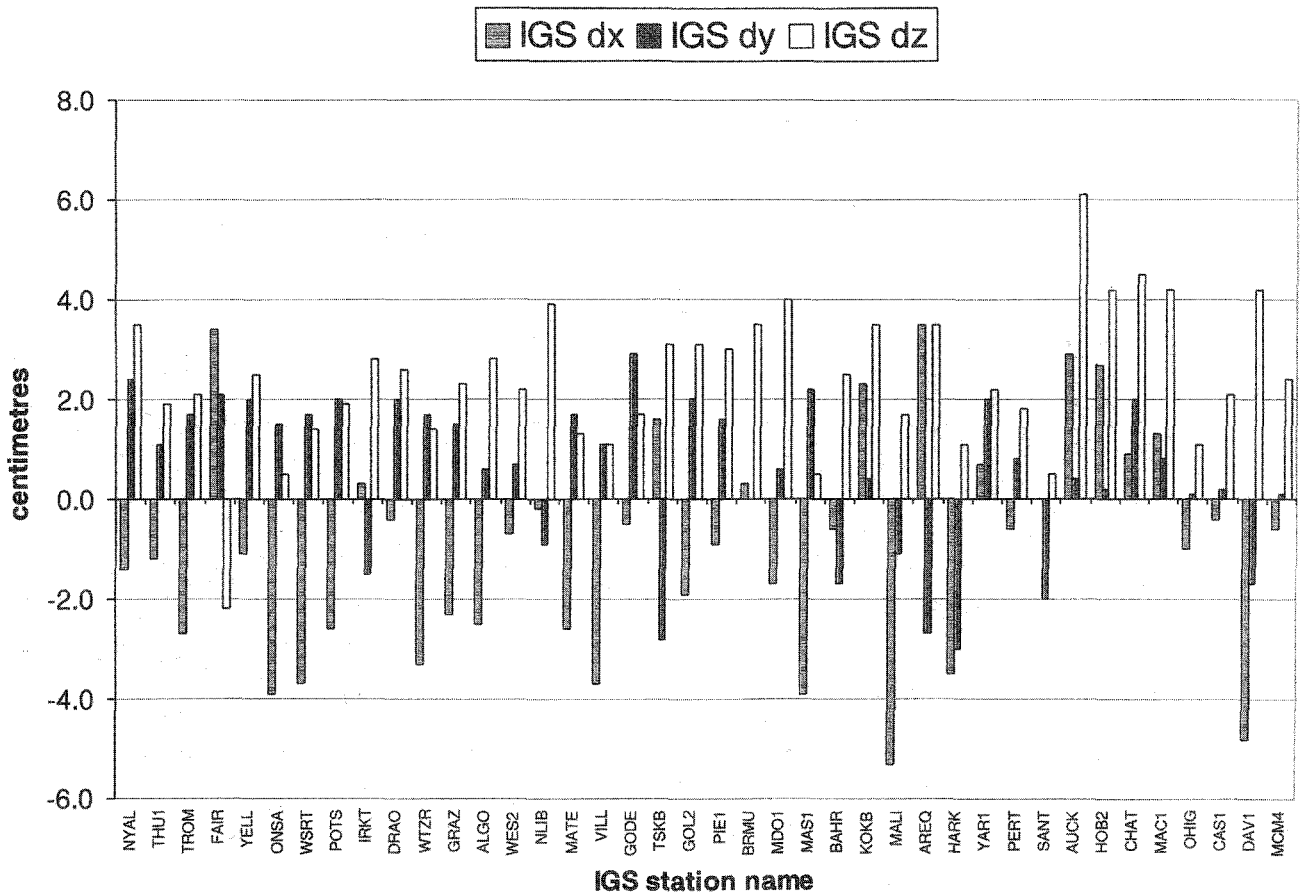


FIGURE 4(a). Precise point positioning with EMR final orbits/clocks-ITRF position differences (cm), 11 December 1999.



**FIGURE 4(b). Precise point positioning with IGS final orbits/clocks -ITRF position differences (cm), 11 December 1999.**

interesting to note that the IGS Rapid product (IGR) is of comparable quality to the IGS Final and the best AC Final orbit/clock products.

In Table 2, the daily average “apparent geocenter offsets” were removed from all the station Cartesian coordinate differences before transforming them into ellipsoidal. After removing the offsets, daily average ellipsoidal coordinate differences are below 2 cm for all centers. A negative height bias of about 1 cm is present for all AC and IGS orbit/clock products. This bias is consistent with a  $-2$ -ppb bias typically seen in all IGS/AC final station solutions (Ferland, 2000). In terms of precision, we obtain fairly consistent standard deviations about the mean for all ACs over the entire week. As expected, the horizontal components are approximately two times more precise than the vertical. Because the standard deviations are with respect to an average difference computed from 35–40 stations, it is affected by regional inconsistencies/biases in the global network. If we consider the standard deviation about the weekly

average on a per station basis, we obtain a 7-day repeatability precision that is approximately two times better (see Table 2). This is consistent with PPP repeatability results obtained with other software using other orbit/clock solutions (e.g., Zumberge et al., 1997).

### Tropospheric Zenith Path Delay Precision Evaluation

In addition to the station position and clock unknowns, the station tropospheric zenith path delays (zpd) are estimated at 15-min intervals. As for station coordinates, zpd estimates require a certain time to converge when the adjustment procedure is initiated using unconstrained parameters. One way of recovering the final zpd estimates (as well as station clocks) for all epochs is to smooth the parameters by a backward substitution with the final converged satellite ambiguity parameters held fixed. This approach, which approximates a rigorous backward filter (or back substitution in a batch least square processing), was implemented in the software to obtain nearly optimal station zpd (and station clock off-

**TABLE 1**

**Daily average cartesian coordinate differences and standard deviations, GPS week 1039**

		<i>Average <math>\Delta x, \Delta y, \Delta z</math> (cm)</i>														
<i>Date</i>	<i>#Stn</i>	<i>EMR</i>			<i>GFZ</i>			<i>IGR</i>			<i>IGS</i>			<i>JPL</i>		
		$\Delta x$	$\Delta y$	$\Delta z$	$\Delta x$	$\Delta y$	$\Delta z$	$\Delta x$	$\Delta y$	$\Delta z$	$\Delta x$	$\Delta y$	$\Delta z$	$\Delta x$	$\Delta y$	$\Delta z$
05-Dec-99	34	1.7	2.4	10.0	-0.5	0.3	0.8	0.2	-0.9	1.1	0.1	0.5	2.0	-1.3	-0.6	4.1
06-Dec-99	32	1.3	-0.1	-4.1	0.1	0.1	0.9	0.0	0.0	0.9	0.0	0.0	0.9	-0.8	-0.8	4.7
07-Dec-99	35	1.6	2.7	7.1	-0.4	0.0	1.0	-0.4	0.1	0.7	-0.3	0.4	1.9	-1.0	-1.4	4.7
08-Dec-99	38	-1.2	-0.1	3.8	-0.2	0.1	1.2	0.2	0.1	0.8	-0.1	-0.1	2.0	-1.5	-0.9	4.4
09-Dec-99	39	-2.0	0.2	10.8	0.1	0.1	1.0	0.1	0.1	1.2	-0.1	-0.1	2.6	-1.1	-0.9	4.7
10-Dec-99	39	1.4	0.7	2.7	0.0	-0.1	1.2	0.1	-0.2	1.1	0.2	0.3	1.8	-1.0	-1.2	4.9
11-Dec-99	40	-3.3	2.8	15.4	0.0	0.1	1.3	0.2	-0.1	1.0	-1.0	0.6	2.4	-1.4	-0.7	4.5

		<i>Standard Deviation (about the mean in cm)</i>														
<i>Date</i>	<i>#Stn</i>	<i>EMR</i>			<i>GFZ</i>			<i>IGR</i>			<i>IGS</i>			<i>JPL</i>		
		$\sigma x$	$\sigma y$	$\sigma z$	$\sigma x$	$\sigma y$	$\sigma z$	$\sigma x$	$\sigma y$	$\sigma z$	$\sigma x$	$\sigma y$	$\sigma z$	$\sigma x$	$\sigma y$	$\sigma z$
05-Dec-99	34	1.5	2.3	1.7	1.7	2.0	1.3	1.9	1.8	1.5	1.5	2.1	1.4	1.9	2.3	1.4
06-Dec-99	32	2.3	2.2	1.6	2.1	1.9	1.2	2.3	2.1	1.2	1.9	2.0	1.2	2.1	2.3	1.3
07-Dec-99	35	2.4	2.5	1.6	2.3	2.2	1.3	2.2	1.9	1.6	1.9	2.0	1.4	2.6	2.8	1.8
08-Dec-99	38	2.3	2.9	1.8	1.8	1.7	1.4	1.8	1.9	1.6	1.7	1.9	1.4	1.9	2.1	1.6
09-Dec-99	39	2.1	2.1	1.3	2.4	1.7	1.3	1.7	1.8	1.5	2.4	1.5	1.4	2.5	2.1	1.8
10-Dec-99	39	1.8	2.3	1.7	1.9	1.6	1.5	1.7	2.0	1.8	1.9	1.8	1.6	1.9	2.1	1.8
11-Dec-99	40	2.4	2.2	1.6	2.1	1.7	1.3	2.7	2.0	1.4	2.2	1.6	1.4	2.1	2.1	1.2

set) time series based on all observations within the observation session (e.g., 24 h). Without such a back substitution scheme only the parameter solutions of the last epoch are optimal.

To evaluate the quality and consistency of our approach, the estimated zpds for week 1039 using orbit products from different ACs were compared with the IGS combined tropospheric product (Gendt, 1998). IGS presently combines zpds at 2-h intervals from contributions made by the seven ACs for up to 200 globally distributed GPS tracking stations. The IGS combined station

zpds have been compared with estimates derived from other techniques and have proven to be quite precise (~7–8 mm) and accurate (Gendt, 1996).

Figure 5 shows a 7-day time series of zpds obtained with a PPP for station YELL during GPS week 1039 using precise orbit products from EMR, GFZ, JPL, IGS, and IGR. The IGS combined estimates (CMB) are also included. A general agreement between all time series is obvious.

To get a more global view of the quality of the zpd estimates, the daily means and standard deviations of differences with respect to the 2-h IGS combined esti-

**TABLE 2**

**Weekly average ellipsoidal differences and standard deviations, GPS week 1039**

	<i>EMR</i>			<i>GFZ</i>			<i>IGR</i>			<i>IGS</i>			<i>JPL</i>		
	$\phi$	$\lambda$	$\eta$	$\phi$	$\lambda$	$\eta$	$\phi$	$\lambda$	$\eta$	$\phi$	$\lambda$	$\eta$	$\phi$	$\lambda$	$\eta$
Average	0.6	0.4	-1.7	0.1	0.2	-1.3	0.2	0.7	-0.9	0.4	0.1	-1.2	0.4	0.4	-1.3
Standard Deviation	1.1	1.6	2.3	1.1	1.4	2.1	1.2	1.5	2.2	1.1	1.4	2.1	1.2	1.6	2.4
7-Day Repeatability	0.6	0.8	1.4	0.3	0.6	1.0	0.5	1.0	1.4	0.4	0.7	1.4	0.5	0.8	1.5

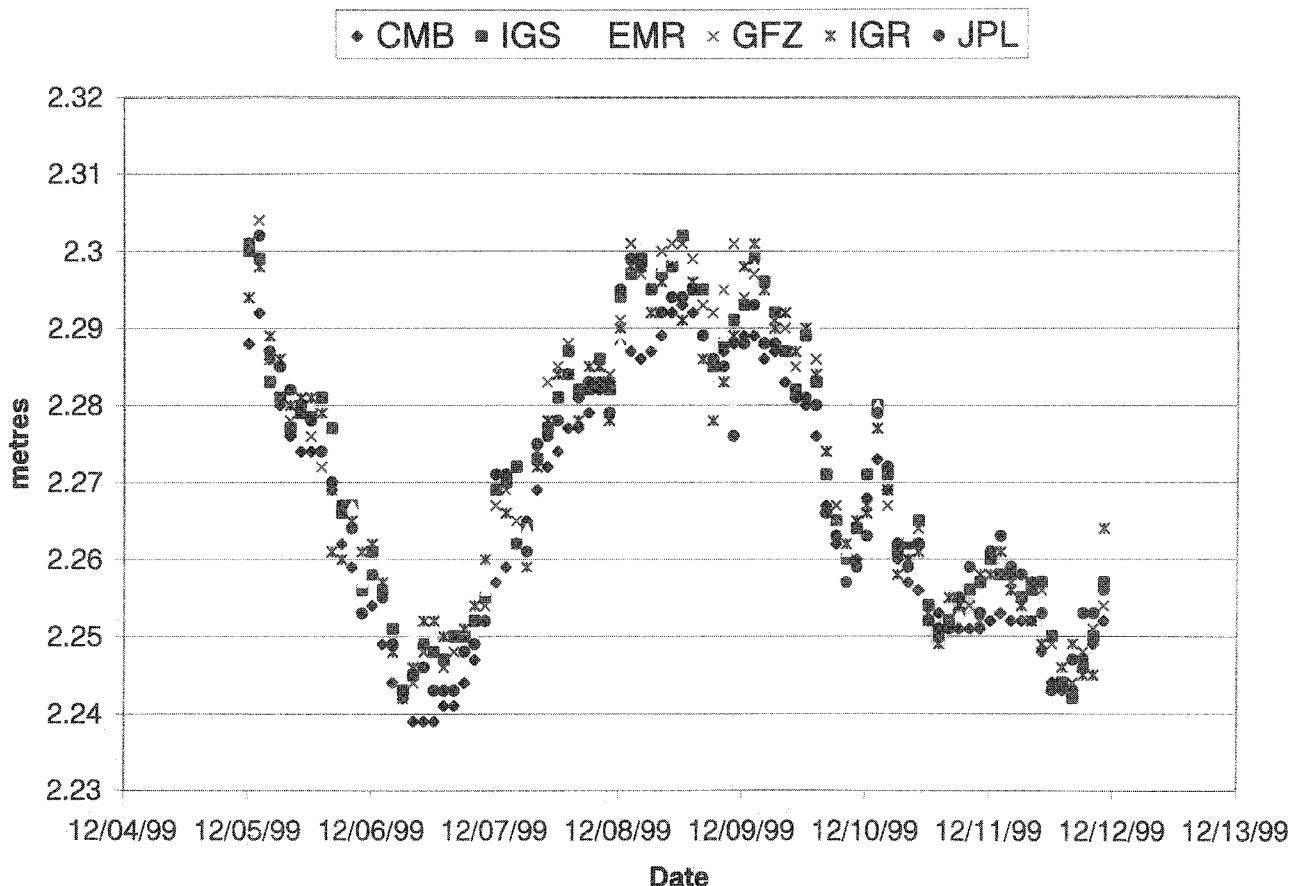


**FIGURE 5. IGS combined (CMB) tropospheric zpd solutions at station YELL and PPP zpd solutions (in meters) using IGS, IGR, GFZ, and JPL orbit/clock products.**

mates are summarized in Table 3. These values were obtained from daily comparisons of approximately 30 IGS stations over the 7 days of GPS week 1039. There are no apparent biases in the means and standard deviations vary from 5 to 8 mm, corresponding to about 1 mm of integrated precipitable water (IPW).

### PPP Station Clock Precision Evaluation

Evaluating the quality of PPP estimated station clocks is somewhat complicated by the absence of an absolute standard for comparison and the fact that different reference clocks and alignment values are used by the ACs in the computation of their daily solutions. Therefore, the following evaluation is an internal comparison between the station clocks estimated with PPP and those produced by GFZ, JPL, and EMR analysis centers (ACs).

Station Wetzell (WTZR) was selected for clock comparison since it is equipped with a Hydrogen MASER (HM) clock and processed by the three selected ACs for most days of GPS week 1039. The WTZR station clock

solutions were extracted from daily station/satellite clock files submitted by EMR, GFZ, and JPL in support of the IGS/BIPM precise timing pilot project (Ray, 1998). Table 4 shows the reference clock used by each AC in their daily clock computation. Note that the two reference stations (ALGO, NRC1) are also equipped with high-quality HM clocks. Because of the requirement to set a station clock as reference in the AC network solutions, the WTZR station clock estimates will contain effects from both WTZR and the reference clocks.

To remove the effect introduced by the different reference clocks' offsets and drifts, and to check the solution quality, a daily linear regression was applied to the AC (EMR, GFZ, JPL) and PPP station clock estimates (EMR\_SP3, GFZ\_SP3, JPL\_SP3) for WTZR. Since WTZR and all the clock reference stations are equipped with high-quality HM clocks, 24-h straight-line RMS of fit of only a few cm should be expected. Table 4 gives the daily regression RMS of the WTZR 15-min clock residuals obtained from the AC and PPP processing. These statis-

**TABLE 3****Tropospheric zpd daily average differences and standard deviations with respect to IGS combined zpd (in cm), GPS week 1039**

Date	#Stn	EMR		GFZ		IGR		IGS		JPL	
		$\Delta zpd$	$\sigma zpd$	$\Delta zpd$	$\sigma zpd$	$\Delta zpd$	$\sigma zpd$	$\Delta zpd$	$\sigma zpd$	$\Delta zpd$	$\sigma zpd$
05-Dec-99	28	-0.3	0.7	-0.2	0.6	-0.5	0.7	-0.3	0.7	-0.2	0.6
06-Dec-99	28	-0.1	0.7	-0.2	0.6	-0.2	0.6	-0.1	0.6	0.0	0.8
07-Dec-99	31	-0.2	0.7	-0.1	0.7	-0.1	0.8	-0.1	0.7	-0.1	0.7
08-Dec-99	32	0.0	0.6	0.1	0.6	0.0	0.7	0.1	0.8	0.0	0.7
09-Dec-99	32	-0.3	0.6	-0.2	0.5	-0.2	0.7	-0.1	0.6	-0.5	0.6
10-Dec-99	33	0.0	0.7	0.1	0.7	0.3	0.7	0.1	0.7	0.1	0.6
11-Dec-99	32	-0.1	0.8	0.1	0.7	-0.2	0.9	0.0	0.8	-0.2	0.6

tics show that the AC and PPP solutions of the WTZR clock have regression RMS at the 3–6-cm level (100–200 ps), which is consistent with the expected HM clock stability at or below  $10^{-14}/100$  s. It is interesting to note that even though the IGS statistics for the quality of the AC satellite clock solutions (as reported in igs10397.sum) vary from 15 cm to 3 cm, the WTZR station clock obtained from PPP with the AC orbits/clock products is of comparable quality.

Figure 6 shows the residuals for the six different solutions over the 7 days of week 1039. There is a systematic effect with peak-to-peak amplitude of ~20 cm (0.6 ns) that corresponds well to what is expected from station GPS antenna cable temperature sensitivity (Larson, 2000). The AC and PPP solutions both contain the effects

of such unmodeled temperature variations affecting the WTZR and the reference clocks (i.e., ALGO or NRC1). In this instance, no detectable temperature-related clock variations are expected from ALGO or NRC1 since at both sites the antenna cables are shielded from the local environment.

10 and 11 December are the only two days of week 1039 where WTZR clock solutions are available from the three ACs as a common reference. For those days, the linear regression residuals from the different solutions were differenced with respect to a particular AC to cancel out the common signal (e.g., temperature variation, HM clock instabilities) in order to assess the quality of the different solutions. Figure 7 shows the differenced WTZR clock residuals for five solutions with respect to GFZ. In

**TABLE 4****Daily regression RMS of 15-min clock residuals for station WTZR, GPS week 1039**

Date	EMR				GFZ				JPL			
	Ref Clock	SP3 Satellite Clock RMS (cm)	AC-WTZR Clock RMS (cm)	PPP WTZR Clock RMS (cm)	Ref Clock	SP3 Satellite Clock RMS (cm)	AC-WTZR Clock RMS (cm)	PPP WTZR Clock RMS (cm)	Ref Clock	SP3 Satellite Clock RMS (cm)	AC-WTZR Clock RMS (cm)	PPP WTZR Clock RMS (cm)
05-Dec-99	NRC1	15	4.0	4.0	ALGO	3	3.3	3.6	ALGO	12	4.0	6.2
06-Dec-99	ALGO	15	2.7	4.0	ALGO	6	2.9	3.1	ALGO	12		
07-Dec-99	ALGO	15	2.0	4.0	ALGO	3	3.3	3.3	ALGO	15		
08-Dec-99	NRC1	15	3.3	4.6	ALGO	3	2.0	3.6	NRC1	12	3.4	6.3
09-Dec-99	NRC1	15	5.1	4.6	ALGO	3	3.8	4.1	ALGO	12	3.1	2.7
10-Dec-99	ALGO	12	3.7	5.3	ALGO	3	4.0	5.1	ALGO	12	3.4	6.2
11-Dec-99	ALGO	18	3.2	3.9	ALGO	3	3.7	4.1	ALGO	15	2.9	2.4

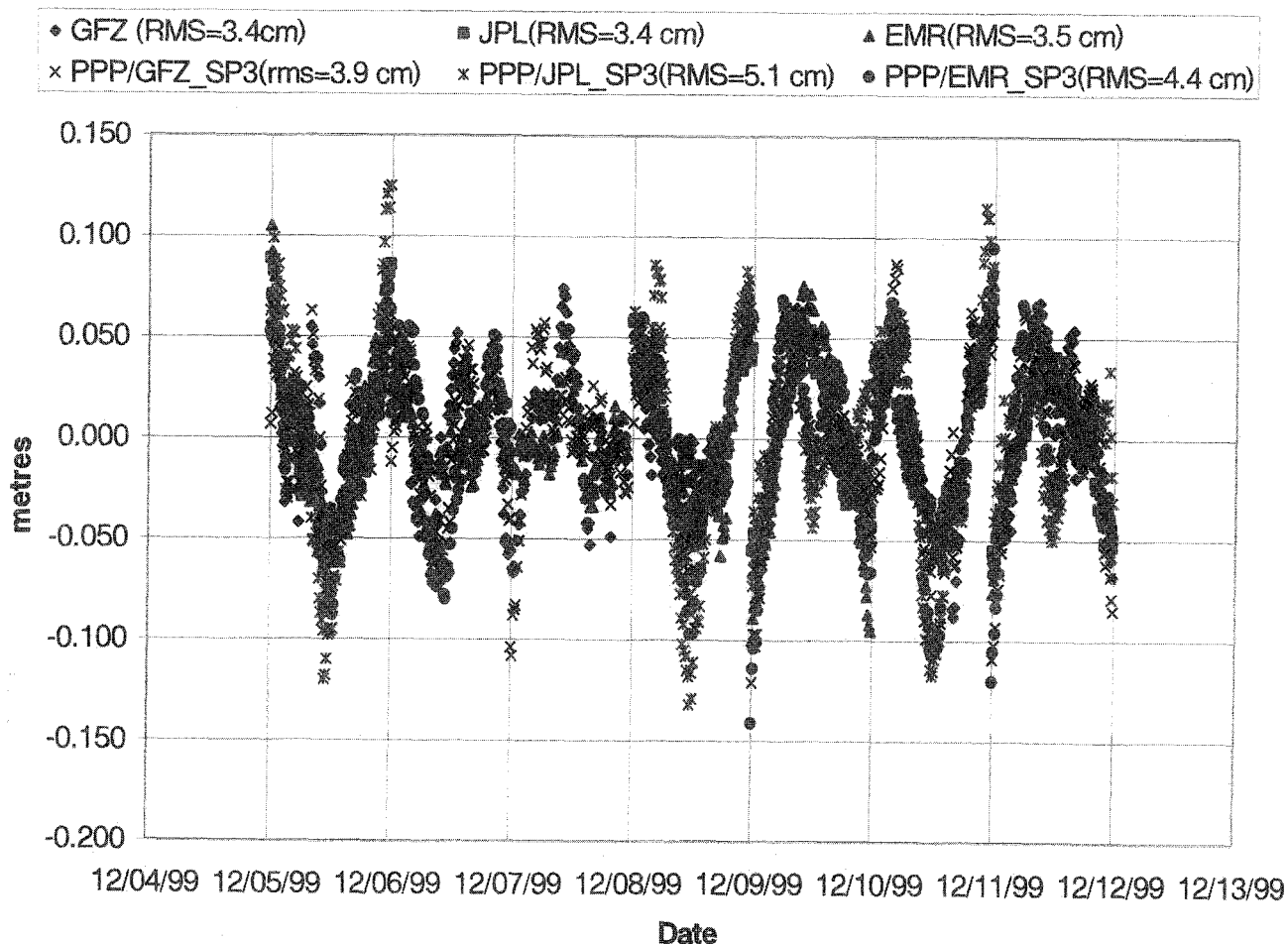


**FIGURE 6. 24-h linear regression clock residuals from AC and PPP estimates for station WTZR clock, GPS week 1039.**

comparison to the undifferenced clocks, there is a definite reduction in the RMS from the 3–6 cm to the 1.3–3 cm (40–100 ps) level. Nevertheless, there are still some systematic effects noticeable in the time series (and Table 4), mainly in the PPP estimates, possibly because no PPP clock weighting was employed. This requires further investigation.

## CONCLUSIONS

The observation equations, estimation technique, and station/satellite models used for the implementation of GPS precise point positioning using IGS orbit/clock products were described. A post-processing approach that uses dual-frequency pseudorange and carrier phase observations from a single GPS receiver and estimates station coordinates, tropospheric zenith path delays, and clock parameters was developed and tested. Results show that global centimeter positioning precision can be real-

ized, directly in ITRF, when using precise orbits/clock products from different IGS Analysis Centers (ACs) and the IGS combinations. The results also indicate that the station position repeatability of our implementation is comparable to PPP repeatability typically obtained when using a consistent set of software for both clock/orbit determination and subsequent PPP. The PPP results also reveal the existence of apparent geocenter offsets between orbit products from different ACs. Furthermore, station tropospheric zenith path delays with centimeter precision and GPS receiver clock estimates precise to 100 ps can also be obtained using this technique. The simple PPP mode presented here forms an ideal interface to the IGS orbit/clock products and ITRF as it can be ported to a personal computer and executes with minimum user intervention. The approach is equally applicable to global kinematic positioning/navigation at the cm-dm level as is being demonstrated daily within IGS combination

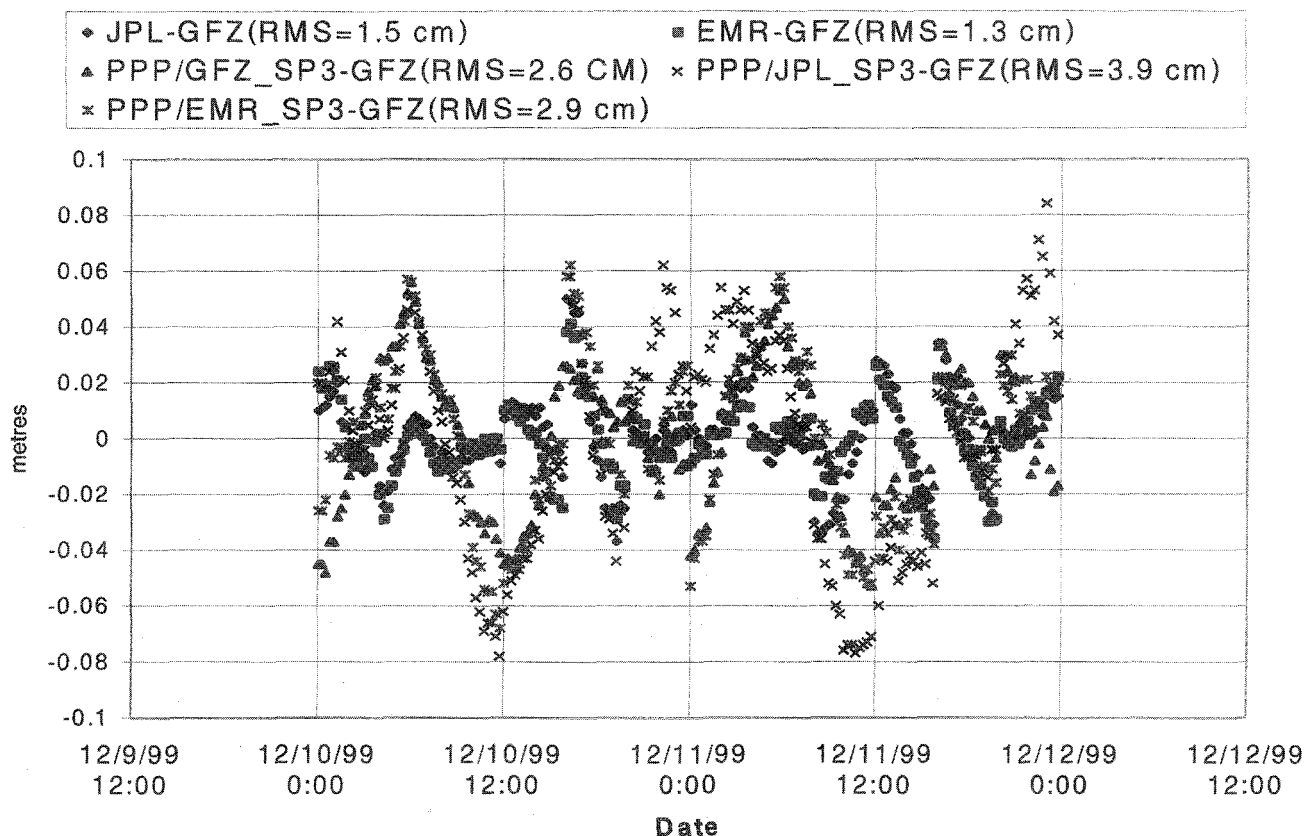


**FIGURE 7. Differenced clock residuals from AC and PPP estimates for station WTZR, 10–11 December 1999.**

summary reports (see IGS Rapid and Final Combination Summary Reports at the IGS CB archives: <http://igs.cb.jpl.nasa.gov/mail/igsreport/igsreport.html>). Furthermore, now that Selective Availability (SA) has been permanently switched off, the 5-min IGS combined clock products can be interpolated at cm-dm precision (Zumberge & Gent, 2000) and PPP (static/kinematic) can be used to process GPS data observed at any sampling interval to achieve cm to dm global positioning.

### ACKNOWLEDGMENTS

The authors are grateful to the many individuals and organizations worldwide who contribute to the International GPS Service. IGS data and products are the result of an unprecedented voluntary, yet coordinated effort that continues to provide an invaluable service to the scientific community. The authors are indebted to J.F. Zumberge of JPL and another anonymous reviewer for their valuable reviews, comments, and suggestions.

### REFERENCES

Agnew, D.C. (1996). SPOTL: Some programs for ocean-tide loading. SIO Ref. Ser. 96-8, Scripps Institution of Oceanography, La Jolla, California.

Bar-Sever, Y.E. (1996). A new model for GPS yaw attitude. *Journal of Geodesy*, 70, 714–723.

Dong, D., et al. (1997). Geocenter variations caused by atmosphere, ocean and surface ground water. *GRL*, 25(15), 1867–1870.

Dragert, H., James, T.S., & Lambert, L. (2000). Ocean loading corrections for continuous GPS: A case study at the Canadian coastal site Holberg. *Geophysical Research Letters*, 27(14), 2045–2048.

Ferland, R. (1999). ITRF Coordinator report. In: IGS annual report.

Gendt, G. (1996). Comparison of IGS troposphere estimations. In R.H. Neilan, P.A. Van Scoy, & J.E. Zumberge (Eds.), *Proceedings of 1996 IGS Analysis Center Workshop* (pp. 151–164). Pasadena, CA: IGS Central Bureau, Jet Propulsion Laboratory.

Gendt, G. (1998). IGS combination of tropospheric estimates—Experience from pilot experiment. In J.M. Dow, J. Kouba, & T. Springer (Eds.), *Proceedings of 1998 IGS Analysis Center Workshop* (pp. 205–216). Pasadena, CA: Jet Propulsion Laboratory.

Héroux, P., Caissy, M., & Gallace, J. (1993). Canadian active control system data acquisition and validation. In *Proceedings of the 1993 IGS (International GPS Service for Geodynamics) Workshop* (pp. 49–58). University of Berne.

Héroux, P., & Kouba, J. (1995, June). GPS precise point positioning with a difference. Paper presented at Geomatics '95, Ottawa, Ontario, Canada.

IERS. (1989). IERS standards (1989). IERS Technical Note 3 (D.D. McCarthy, Ed.). IERS Central Bureau, Observatoire de Paris.

IERS. (1996). IERS conventions (1996). IERS Technical Note 21 (D.D. McCarthy, Ed.). IERS Central Bureau, Observatoire de Paris.

ION. (1980). *Global positioning system. Vol. 1. Papers published in "Navigation."* The Institution of Navigation, Alexandria, VA.



- King, R.W., & Bock, Y. (1999). Documentation of the GAMIT GPS Analysis Software (version 9.8). Unpublished paper. Massachusetts Institute of Technology, Cambridge, MA.
- Kouba, J. (1998). IGIS analysis activities (1998). In IGS annual report (pp. 13–17). Pasadena, CA: IGS Central Bureau, Jet Propulsion Laboratory.
- Kouba, J., Mireault, Y., Beutler, G., & Springer, T. (1998). A discussion of IGS solutions and their impact on geodetic and geophysical applications. *GPS Solutions*, 2(2), 3–15.
- Larson, K.M., Levine, J., & Nelson, I.M. (2000). Assessment of GPS phase stability for time-transfer applications. *IEEE Transactions on Ultrasonics, Ferroelectrics and Frequency Control*, 47(2), 484–493.
- Lichten, S.M., Bar-Sever, Y.E., Bertiger, E.I., Heflin, M., Hurst, K., Muellerschoen, R.J., Wu, S.C., Yunck, T.P., & Zumberge, J.F. (1995, October). GIPSY-OASIS II: A high precision GPS data processing system and general orbit analysis tool. Presented at Technology 2006: NASA Technology Transfer Conference. Chicago, IL.
- Neilan, R.E., Zumberge, J.E., Beutler, G., & Kouba, J. (1997). The International GPS Service: A global resource for GPS applications and research. In *Proceedings of ION-GPS-97* (pp. 883–889). The Institute of Navigation.
- Pagiatakis, S.D. (1992). Program LOADSDP for the calculation of ocean load effects. *Manuscripta Geodaetica*, 17, 315–320.
- Rothacher, M., & Mervart, L. (1996). *The Bernese GPS Software Version 4.0*. Berne: University of Berne, Astronomical Institute.
- Scherneck, H.G. (1991). A parameterized solid earth tide model and ocean tide loading effects for global geodetic baseline measurements. *Geophysical Journal International*, European Geophysical Society., 106, 677–694.
- Scherneck, H.G. (1993). Ocean tide loading: Propagation errors from ocean tide into loading coefficients. *Manuscripta Geodaetica*, 18, 59–71.
- Wahr, J.M. (1981). The forced nutation of an elliptical, rotating, elastic, and oceanless Earth. *Geophysical Journal of Royal Astronomical Society. (London) Soc.*, 64, 705–727.
- Wu, J.T., Wu, S.C., Hajj, G.A., Bertiger, W.I., & Lichten, S.M. (1993). Effects of antenna orientation on GPS carrier phase. *Manuscripta Geodaetica*, 18, 91–98.
- Zumberge, J.F. (1999). Automated GPS Data Analysis Service. *GPS Solutions*, 2(3), 76–78.
- Zumberge, J.E., & Gent, G. (2000). The Demis of selective availability and implication for the International GPS Service. Position paper presented at the IGS Network Workshop 2000.
- Zumberge, J.E., Heflin, M.B., Jefferson, D.C., Watkins, M.M., & Webb, E.H. (1997). Precise point positioning for the efficient and robust analysis of GPS data from large networks. *Journal of Geophysical Research*, 102, 5005–5017.

## BIOGRAPHIES

Jan Kouba, DrSc, has been working in satellite geodesy since 1970. During 1994–1998 he was the first IGS Analysis Center Coordinator. Although he retired from his active duties at the Geodetic Survey Division of Natural Resources Canada in April 1998 and from the IGS Governing Board in December 1999, he has kept his interest and links with both organizations.

Pierre Héroux, M.Sc., has over 20 years experience in GPS positioning for applications in geodesy and navigation and is currently team leader of the Active Control Systems Technology group at the Geodetic Survey Division of Natural Resources Canada.